Stimulated Emission from the Biexciton in a Single Self-Assembled II-VI Quantum Dot

I. A. Akimov, J. T. Andrews, and F. Henneberger
Institut für Physik, Humboldt Universität zu Berlin, Newtonstrasse 15, 12489 Berlin, Germany
(Received 28 June 2005; published 14 February 2006)

Using two-photon excitation, stimulated emission from the biexciton state in a single CdSe/ZnSe quantum dot is observed in a two-pulse configuration. We directly time resolve the emission-absorption characteristics and verify the potential for laser action. By setting the polarization of the stimulation pulse, the recombination path of the biexciton and, by this, the state of the photons emitted in the decay cascade is controlled. We elaborate also the coherent response and address entanglement and disentanglement of the exciton-biexciton system.

DOI: 10.1103/PhysRevLett.96.067401 PACS numbers: 78.67.Hc, 42.50.Md, 78.55.Et

Semiconductor quantum dots (QDs) with electronic excitations localized on a nanometer length scale have recently attracted much attention as laser units, nonclassical light emitters, as well as building blocks for quantum logic [1]. In all these issues, the biexciton plays a central role. Two-particle interactions are significantly involved in the laser action under three-dimensional carrier confinement [2]. In the spontaneous emission cascade of the biexciton, two photons are emitted that can be polarization correlated or even entangled [3]. Finally, the biexciton itself represents an entangled state that allows one to implement elementary two-quantum bit operations [4].

In general, the biexciton state in QDs is well documented by various experimental studies. However, by far the major part of previous work relies on ensemble averages [5] or nonresonant excitation of the biexciton by pumping into the energy continuum of the QD structure [6]. In order to elucidate the true quantum dynamics, direct resonant excitation of the biexciton is required. In what follows, we present a novel two-photon, two-pulse technique that enables us to control the recombination path of the biexciton and to monitor directly stimulated emission on a single-quantum level.

The two-exciton subspace of a QD is spanned by the ground state $|g\rangle$ (no exciton), the single-exciton states, and the biexciton state $|b\rangle$. The optically active exciton is split by anisotropy in two linearly cross-polarized components $|x\rangle$ and $|y\rangle$ [7] so that the V-Λ transition scheme of Fig. 1(a) is formed. The exciton-biexciton resonances are low-energy shifted from that of the single excitons by the exciton-exciton interaction energy ΔE_{XX} in the biexciton. Excitation of the biexciton $|g\rangle \rightarrow |b\rangle$ requires two photons. Two nondegenerate optical beams, each being resonant to one of the single-photon transitions, e.g., $|g\rangle \rightarrow |x\rangle$ and $|x\rangle \rightarrow |b\rangle$, have been utilized to generate directly biexcitons localized at interface fluctuations of GaAs quantum wells [4,8]. Instead, the present study is based on resonant two-photon (TP) excitation [9,10]. This approach, where the degenerate photons have half the energy of the biexciton, has the important advantage that the spontaneous emission from the cascaded biexciton-exciton decay is clearly separated from the excitation stray light so that one can track the secondary radiation from the QD and make further use of it. In a next step, we accomplish the conversion of the biexciton into an exciton by stimulated emission applying a second pulse that is tuned to the exciton-biexciton resonance. In contrast to the spontaneous emission cascade, the polarization of the stimulation pulse defines strictly along which arm of the transition scheme the exciton-biexciton system recombines. For our goal, wide-band-gap II-VI QDs are especially suited due to their large $\Delta E_{XX} \approx 20$ meV [6], assuring spectral selectivity of the excitation process even when using ultrashort optical pulses.

The Stranski-Krastanov CdSe/ZnSe QD structures are grown by molecular beam epitaxy [11]. In order to study individual QDs, mesa structures with an area down to 100×100 nm^2 are fabricated. The sum frequency of a Kerr-lens mode-locked Ti:sapphire laser and a synchronously pumped optical parametric oscillator are used to generate spectrally broad subpicosecond pulses with

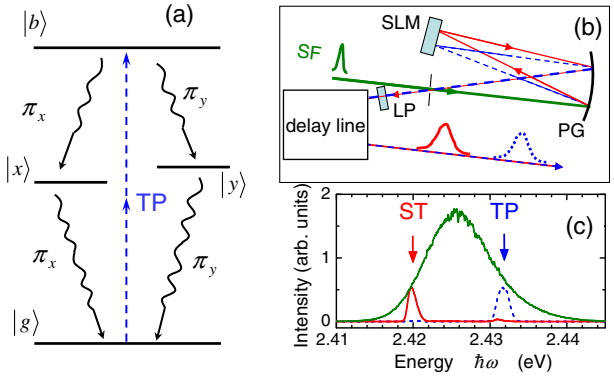

FIG. 1 (color online). (a) Schematics of the exciton-biexciton system in a QD. For explanations, see text. (b) Layout of the pulse shaper. SF, subpicosecond source pulse; SLM, spatial light modulator; PG, parabolic grating; LP, linear polarizer. (c) Spectra of the ingoing SF pulse and the resulting ST and TP pulse.

76 MHz repetition rate in the spectral region of interest. Two spectrally narrow pulses for selective TP excitation and stimulation (ST) of the biexciton are obtained by a pulse shaper based on a programmable reflective spatial light modulator [Fig. 1(b)]. The outgoing pulses are spatially separated and passed through a delay line. The pulse durations are about 1.0 ps (TP) and 1.5 ps (ST) and the spectral full widths at half maximum are 1.7 and 1.2 meV, respectively [Fig. 1(c)]. The secondary emission of the QD is collected in a confocal arrangement and dispersed in a triple spectrometer (0.23 nm/mm) equipped with a nitrogen cooled charged coupled device. For time-resolved measurements, only the two first stages are utilized in subtractive mode (0.7 nm/mm). A multi-channel-plate photomultiplier in conjunction with time-correlated single-photon counting unit provides an overall time resolution of 60 ps. Polarization control is achieved by quarter-wave or half-wave plates, placed in the path of both the linearly polarized excitation light as well as the emission signal. The polarization of the emission is analyzed by a Glan-Thomson prism introduced in front of the spectrometer. All measurements are carried out at temperatures of about 10 K.

The cascaded spontaneous emission of a QD subsequent to TP excitation is depicted in Fig. 2. For linearly polarized excitation, distinct exciton and biexciton features, placed symmetrically to the excitation photon energy, are present. In full accord with the transition scheme of Fig. 1(a), both features consist of a fine structure doublet of linearly cross-polarized lines, however, with a reversed sequence of the polarization in the exciton and biexciton emission. The TP transition of the biexciton is forbidden for circular excitation polarization. While the emission yield indeed decreases by 1 order of magnitude, a weak rest emission at the exciton survives. This background originates probably from electron-hole pairs off-resonantly excited in the energy continuum of the heterostructure and captured by the QD. On the other hand, under linearly polarized excitation, the emission signal at the exciton lines is entirely insensitive on the polarization direction, excluding that the TP pulse addresses directly the exciton states to a measurable extent. A flip between $|x\rangle$ and $|y\rangle$ takes place on a time scale markedly longer than the lifetime and can be thus ignored [12]. The time-resolved emission shown in Fig. 2(b) clearly confirms the existence of an emission cascade, with the biexciton recombining first and with a respective rise time for the exciton [13]. Double-exponential fits yield that the radiative lifetime of the biexciton ($\tau_{XX} = 120$ ps) is about 2 times shorter than for the exciton ($\tau_X = 200$ ps). Since the biexciton has two recombination channels, this means that the exciton and the exciton-biexciton transition posses almost the same dipole moment. Using $d^2 = 3\pi\varepsilon_0\hbar c^3/n_r\omega_0^3\tau$, we find $d = 27$ D.

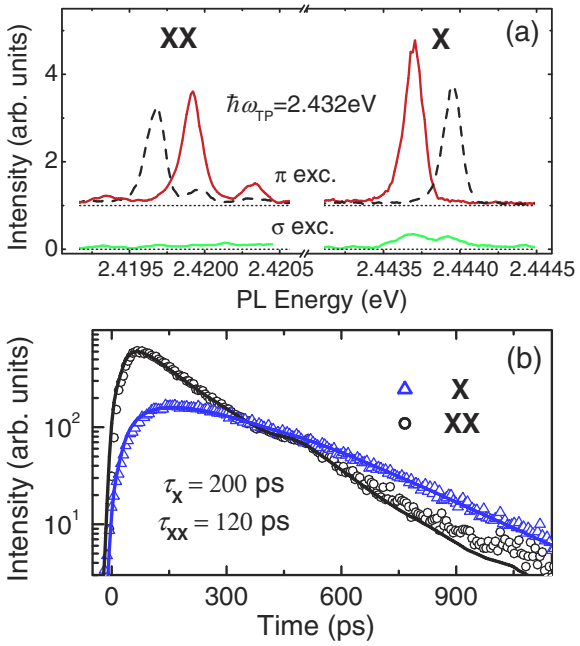

FIG. 2 (color online). (a) Exciton (X) and biexciton (XX) emission lines from a single QD under circularly (σ) and linearly (π) polarized TP excitation. The polarization detection is along (solid lines) and perpendicular to (dashed lines) the intrinsic polarization $\vec{\pi}_x$. (b) Decay transients of biexciton and exciton emission under TP excitation. Solid lines are a double-exponential data fits accounting for the apparatus function.

Now we focus on the stimulated emission of the biexciton. In these measurements, the QD is excited by a sequence of TP and ST pulses, linearly copolarized under an angle φ relative to the intrinsic polarization $\vec{\pi}_x$ and with tunable time delay τ. The result of the stimulation process is a photon as well as an exciton. While the photon can hardly be detected, the stimulated exciton is manifested by the photon that it emits subsequently. The data in Fig. 3(a) directly verify this scenario. While both exciton emission components have almost equal intensity for TP excitation only, the line polarized along the ST polarization is amplified at the expense of the cross-polarized line when both pulses are present. During pulse delay, the biexciton state is increasingly emptied by spontaneous decay. Consistent with the radiative lifetime, the transition is no longer capable of stimulated emission after about 250 ps. A measure to what extend a certain exciton state can be selected by the ST pulse is given by the induced linear polarization degree $\rho_L = (I_x - I_y)/(I_x + I_y)$, I_i being the spectrally integrated exciton signal of $|i\rangle$. As seen in Fig. 3(c), $\rho_L = 0$ for $\varphi = \pi/4$, while exciting along the intrinsic polarization axis ρ_L has the same absolute value but is positive for $\varphi = 0$ and negative for $\varphi = \pi/2$. In an incoherent regime, the polarization degree is limited to $\rho_L = 0.5$, because the inversion between the biexciton and exciton population, addressed for a given ST polarization, cannot exceed zero. In contrast, ρ_L clearly exceeds this limit and reaches values of up to 0.8 for the maximum pulse densities available by our setup. Even the onset of Rabi oscillations for the exciton-biexciton transition is evidenced in Fig. 3(b). The relatively large fine structure

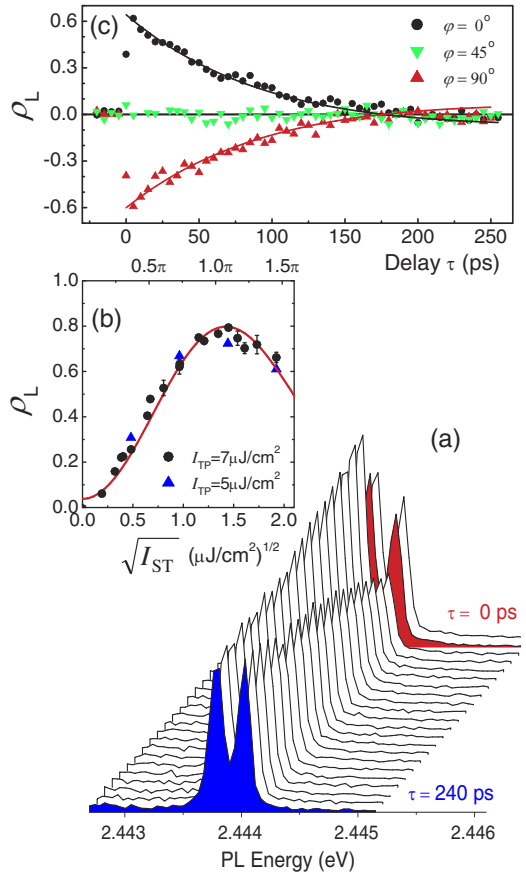

FIG. 3 (color online). (a) Evolution of exciton emission spectrum as a function of the delay τ between TP and ST pulse. The ST polarization is along the polarization of the low-energy line. (b) Induced linear polarization degree ρ_L vs square-root pulse density $\sqrt{I_{\mathrm{ST}}}$ ($\tau = 5$ ps, $\varphi = 0$). (c) ρ_L vs τ for ($I_{\mathrm{TP}} = 7\ \mu\mathrm{J/cm}^2$, $I_{\mathrm{ST}} = 1.3\ \mu\mathrm{J/cm}^2$) $\varphi = \angle(\vec{e}, \vec{\pi}_x)$. Since not related to the intrinsic QD dynamics, the off-resonant background is subtracted in (b) and (c). The solid lines are fits to the data based on the numerical solution of the master equation for the two-exciton density matrix. For details, see text.

splitting of the exciton allows us to spectrally separate spontaneous and stimulated emission. For QDs where the splitting is within the homogeneous width the stimulation process can be also accomplished, but shows up only in the polarization degree.

In order to draw quantitative conclusions on the quantum dynamics behind the experimental observations, the full density matrix of the two-exciton subspace has to be considered. Its time evolution is determined by the master equation $\imath\hbar\dot{\varrho} = [H, \varrho] + \imath\hbar\Gamma[\varrho]$ with the Hamiltonian given in units of $\hbar$ and the rotating-wave approximation by

$$H = \omega_g|g\rangle\langle g| + \omega_x|x\rangle\langle x| + \omega_y|y\rangle\langle y|) + \omega_b|b\rangle\langle b| - \tfrac{1}{2}\{\Omega(t)e^{-i\omega t}[\cos(\varphi)(|x\rangle\langle g| + |b\rangle\langle x|) + \sin(\varphi)(|y\rangle\langle g| + |b\rangle\langle y|)] + \mathrm{H.c.}\}.$$

$\Omega = \frac{d}{\hbar}\mathcal{E}(t)$ is the time-dependent Rabi frequency of the field amplitude $\mathcal{E}(t)$, whereby the same d is taken for all transitions. Expressed in the two-exciton basis, the master equation defines a complete set of differential equations for the 10 independent density matrix elements $\varrho_{ij} = \varrho^*_{ji}$. For the relaxation terms, we use $\langle i|\Gamma[\varrho]|j\rangle = -\Gamma_{ij}\varrho_{ij}$ ($i \neq j$), $\langle b|\Gamma[\varrho]|b\rangle = -\varrho_{bb}/\tau_{XX}$, $\langle i|\Gamma[\varrho]|i\rangle = \varrho_{bb}/2\tau_{XX} - \varrho_{ii}/\tau_X$ ($i = x, y$), and $\dot{\varrho}_{bb} + \dot{\varrho}_{xx} + \dot{\varrho}_{yy} + \dot{\varrho}_{gg} = 0$. The equations are numerically solved for Gaussian pulse shapes assuming $\varrho_{gg} = 1$ and all other $\varrho_{ij} = 0$ before the TP pulse and taking the resultant ϱ_{ij} as initial values for the interaction with the ST pulse. In a time-integrated detection mode, the linear polarization degree is given by $\rho_L = (\delta\varrho_{xx} - \delta\varrho_{yy})/(\delta\varrho_{bb} + \delta\varrho_{xx} + \delta\varrho_{yy})$, $\delta\varrho_{ii}$ denoting the change of the populations generated by both pulses.

Except for the off-diagonal damping rates, all parameters (ΔE_{xx}, $E_x - E_y$, d, τ_{XX}, τ_X) entering the equations are known experimentally. Therefore, though the set is relatively large, the population dynamics is fully defined. Calculating ρ_L as a function of the pulse delay indeed yields perfect agreement with the experimental curves in Fig. 3(c). There is a weak but clearly recognizable sign change at about 200 ps. Here, as the exciton lifetime is the longer one, crossover from stimulated emission to absorption occurs. Population of the exciton state restricts the available exciton-biexciton gain. The experimental data verify that even in the strong-confinement limit $\tau_{XX} \approx \tau_X/2$, stimulated emission is by far dominant.

Next we elaborate the coherent part of the response. Note that the interaction of the ST pulse with the biexciton coherence ϱ_{bg} produces off-diagonal elements ϱ_{xg} or ϱ_{yg} so that the subsequent exciton emission has free-induction decay character. The data exhibit no difference on whether $|x\rangle$ or $|y\rangle$ is addressed. Hence, $\Gamma_{xg} = \Gamma_{yg}$, $\Gamma_{bx} = \Gamma_{by}$, and making the assumption of uncorrelated scattering $\Gamma_{bx} = \Gamma_{xg} + \Gamma_{bg}$, the only two free parameters left are the exciton (Γ_{xg}) and biexciton (Γ_{bg}) decoherence rates. Their values are determined by the density dependence of ρ_L [Fig. 3(b)]. Too large rates spoil rapidly the purity of the TP excitation by single-photon absorption in the tail of the exciton line, resulting in a significant polarization degree even without the ST pulse, while the maximum level of only $\rho_L = 0.8$ signifies the presence of pure dephasing beyond the radiative damping. The fit to the data yields $\Gamma_{xg}^{-1} \approx \Gamma_{bg}^{-1} = 6$ ps. A careful analysis of the spectral line shape of the exciton emission provides that the radiative Lorentzian is superimposed to a weak but broad acoustic phonon background, which translates in nonexponential damping in the time domain with a short component consistent with the rates deduced from the present data (see also [14]). Distinct nonexponential damping is also indicated by TP coherent control measurements [10]. Here, a significant drop of the contrast occurs right after pulse separation, whereas the subsequent decay evolves on a much longer time scale. Figure 4 represents plots of the density matrix elements versus pulse area $\theta = \int_{-\infty}^{+\infty}\Omega(t)dt$ in the experimentally relevant pulse-density range. Despite

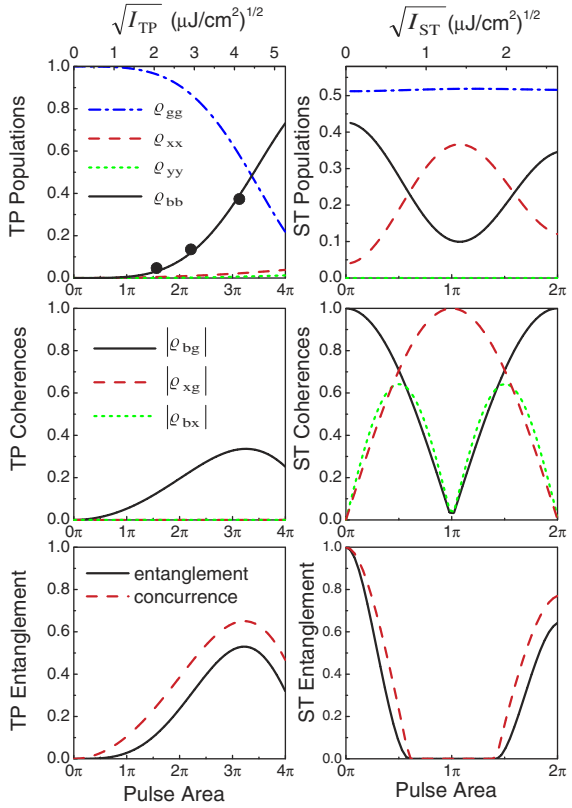

FIG. 4 (color online). Calculated populations, coherences, entanglement, and concurrence versus pulse area for the TP (left) and the ST (right) pulse. The experimental points in the left top panel represent the normalized signal of the XX emission under TP excitation only. The plots in the two lower right panels are normalized with respect to the initial values produced by the TP pulse. $\tau = 5$ ps, $\theta_{TP} = 3\pi$, and $\varphi = 0$.

of the relatively fast dephasing, the TP pulse creates still a significant ϱ_{bg} that is transformed in a respective exciton coherence by the succeeding ST pulse.

In a quantum information sense, the TP excitation creates a Bell-like state $a_{00}|00\rangle + a_{11}|11\rangle$, which is subsequently disentangled in the stimulated emission process. The entanglement of formation $E(\varrho)$ is given by $E = E(C) = h(\frac{1+\sqrt{1-C^2}}{2})$ with the concurrence $C(\varrho) = \max[0, \lambda_1 - \lambda_2 - \lambda_3 - \lambda_4]$ [15]. The λ_i are in decreasing order the square roots of $\varrho\sigma_y \otimes \sigma_y\varrho^*\sigma_y \otimes \sigma_y$ (σ_y, time inversion operator) and $h(x) = -x\log_2(x) - (1-x)\log_2(1-x)$. For a purely coherent regime, it is straightforward to show that $C = 2\sqrt{\varrho_{gg}\varrho_{bb}}$. Knowing the full exciton-biexciton density matrix, E and C can be readily calculated. While a situation close to $\varrho_{bb} \approx \varrho_{gg} \approx \frac{1}{2}$ can indeed be reached by the TP pulse, the maximum entanglement is only about 0.5, showing that a mixed state is merely formed as a result of decoherence. However, given this limitation, complete disentanglement is accomplished by the ST pulse in a wide range of pulse areas (Fig. 4). Optical disentanglement of the exciton-biexciton system has been also demonstrated in Ref. [4]. The present approach is different as it allows for an arbitrary time (within τ_{XX}) to pass after the creation of the biexciton to apply the disentangling pulse.

In summary, we have demonstrated stimulated emission from the biexciton in a single QD by a two-pulse setup. Our findings uncover new information demonstrating the potential of the biexciton state in various regards. We have directly time resolved the emission-absorption characteristics of the exciton-biexciton transition. Although the lifetime relation is not optimum, sufficiently large inversion and thus laser action can be attained. Being able to control the recombination path of the biexciton, the spontaneous cascade emission can be adjusted from a pair of correlated or even entangled photons to a single photon of defined polarization or in an entangled polarization state. The data evidence further a significant coherent contribution associated with excitonic free-induction decay or superradiance in an ensemble of QDs. It can be also utilized for optical entanglement and disentanglement of the electronic states.

The authors thank S. Rogaschewski for the lithographic etching. This work was supported by the Deutsche Forschungsgemeinschaft within Project No. He 1939/18-1.

[1] D. Gammon and D. G. Steel, Phys. Today **55**, No. 10, 36 (2002), and references therein.
[2] F. Kreller *et al.*, Phys. Rev. Lett. **75**, 2420 (1995); V. I. Klimov *et al.*, Science **290**, 314 (2000); A. A. Mikhailovsky *et al.*, Appl. Phys. Lett. **80**, 2380 (2002).
[3] O. Benson *et al.*, Phys. Rev. Lett. **84**, 2513 (2000); C. Santori *et al.*, Phys. Rev. B **66**, 045308 (2002).
[4] X. Li *et al.*, Science **301**, 809 (2003).
[5] P. Borri *et al.*, Phys. Rev. Lett. **89**, 187401 (2002).
[6] V. D. Kulakovskii *et al.*, Phys. Rev. Lett. **82**, 1780 (1999); F. Kreller *et al.*, Appl. Phys. Lett. **74**, 2489 (1999).
[7] D. Gammon *et al.*, Phys. Rev. Lett. **76**, 3005 (1996); M. Bayer *et al.*, Phys. Rev. Lett. **82**, 1748 (1999).
[8] Gang Chen *et al.*, Phys. Rev. Lett. **88**, 117901 (2002).
[9] K. Brunner *et al.*, Phys. Rev. Lett. **73**, 1138 (1994); F. Gindele *et al.*, Phys. Rev. B **60**, 8773 (1999).
[10] T. Flissikowski *et al.*, Phys. Rev. Lett. **92**, 227401 (2004).
[11] D. Litvinov *et al.*, Appl. Phys. Lett. **81**, 640 (2002).
[12] T. Flissikowski *et al.*, Phys. Rev. Lett. **86**, 3172 (2001).
[13] G. Bacher *et al.*, Phys. Rev. Lett. **83**, 4417 (1999); T. H. Stievater *et al.*, Phys. Rev. B **65**, 205319 (2002).
[14] L. Besombes *et al.*, Phys. Rev. B **63**, 155307 (2001); P. Borri *et al.*, Phys. Rev. Lett. **87**, 157401 (2001); E. A. Muljarov and R. Zimmermann, Phys. Rev. Lett. **93**, 237401 (2004).
[15] W. K. Wootters, Phys. Rev. Lett. **80**, 2245 (1998).